Influence of temperature and exploitation period on fatigue crack growth parameters in different regions of welded joints

Ivica Camagic, Nemanja Vasic, Bogdan Cirkovic
Faculty of Technical Sciences, Kosovska Mitrovica, Kneza Milosa 7, Serbia

Zijah Burzic
Military Technical Institute, Rastka Resanovica 1, Belgrade, Serbia

Aleksandar Sedmak
Faculty of Mechanical Engineering, Kraljice Marije 16, Belgrade, Serbia
asedmak@mas.bg.ac.rs

Aleksandar Radovic
Technical School Mihailo Petrovic Alas, Kosovska Mitrovica, Lole Ribara 29, Serbia

ABSTRACT. The influence of exploitation period and temperature on the fatigue crack growth parameters in different regions of a welded joint is analysed for new and exploited low-alloyed *Cr-Mo* steel A-387 *Gr. B*. The parent metal is a part of a reactor mantle which was exploited for over 40 years, and recently replaced with new material. Fatigue crack growth parameters, threshold value ΔK_{th}, coefficient C and exponent m, have been determined, both at room and exploitation temperature. Based on testing results, fatigue crack growth resistance in different regions of welded joint is analysed in order to justify the selected welding procedure specification.

KEY WORDS: Welded joint; Crack; Yield stress; Tensile strength; Permanent dynamic strength.

INTRODUCTION

The reactor analysed here has a form of a vertical pressure vessel with a cylindrical mantle and two welded lids, made of *Cr-Mo* steel A-387 *Gr. B*, [1]. It is used for some of the most important processes in the motor gasoline production, including platforming in order to change the structure of hydrocarbon compounds and to achieve a higher octane rating. Long-time, high temperature exploitation of the reactor, caused siginficant damage in reactor mantle, requiring a thorough inspection and repair of damaged parts, including replacement of a part of reactor mantle. For designed exploitation parameters (p=35 bar, t=537 °C), the material is prone to decarbonization, reducing its strength as a consequence, [2]. Testing of high-cycle fatigue behaviour of new and exploited parent metal (PM), weld metal (WM) and heat affected zone (HAZ), at room and service temperature (540 °C) is necessary to get detailed insight in all parameters influencing fatigue crack growth resistance of *Cr-Mo* steel A-387 *Gr. B*. welded joints.

TESTING MATERIAL

Both new and exploited PM was steel A-387 *Gr. B* with thickness of 102 mm. Chemical composition and mechanical properties for both new and exploited PM are given in Tabs. 1 and 2.

Specimen designation	% max							
	C	Si	Mn	P	S	Cr	Mo	Cu
E	0.15	0.31	0.56	0.007	0.006	0.89	0.47	0.027
N	0.13	0.23	0.46	0.009	0.006	0.85	0.51	0.035

Table 1: Chemical composition of exploited (E) and new (N) PM specimens

Specimen designation	Yield stress, $R_{p0.2}$, MPa	Tensile strength R_m, MPa	Elongation A, %	Impact energy, J
E	320	450	34.0	155
N	325	495	35.0	165

Table 2: Chemical composition of exploited (E) and new (N) PM specimens.

Welding of both new and exploited PM was performed in two stages, according to the following welding procedure specification:

- Root pass by shielded metal arc welding, using LINCOLN S1 19G electrode, and
- Filling passes by arc submerged arc welding, using LINCOLN LNS 150 wire and LINCOLN P230 flux.

Chemical composition of the coated electrode LINCOLN S1 19G, and the wire LINCOLN LNS 150 according to the atest documentation is given in tab. 3, whereas their mechanical properties, also according to the atest documentation, are given in tab. 4.

Filler material	% mas						
	C	Si	Mn	P	S	Cr	Mo
LINCOLN S1 19G	0.07	0.31	0.62	0.009	0.010	1.17	0.54
LINCOLN LNS 150	0.10	0.14	0.71	0.010	0.010	1.12	0.48

Table 3: Chemical composition of filler materials.

Filler material	Yield stress, $R_{p0.2}$, MPa	Tensile strength R_m, MPa	Elongation A, %	Impact energy, J, 20°C
LINCOLN S1 19G	515	610	20	>60
LINCOLN LNS 150	495	605	21	>80

Table 4: Mechanical properties of filler materials

FATIGUE CRACK GROWTH PARAMETERS EVALUATION

Fatigue crack growth testing at room temperature was performed on three-point bending specimens, as defined by ASTM E399, [3], whereas tesitng at service temperature, 540 °C, was performed on modified CT specimens, as defined by standard BS 7448 Part 1, [4]. The high-frequency resonant pulsator was used, in force control mode, with loading ratio R = 0.1 to obtain diagrams da/dN-ΔK for specimens with fatigue crack tip located in PM, WM and

HAZ, both new and expoloited material, at room and service temperature. Only two diagrams are shown here, as an illustration, whereas the others can be found in [1].

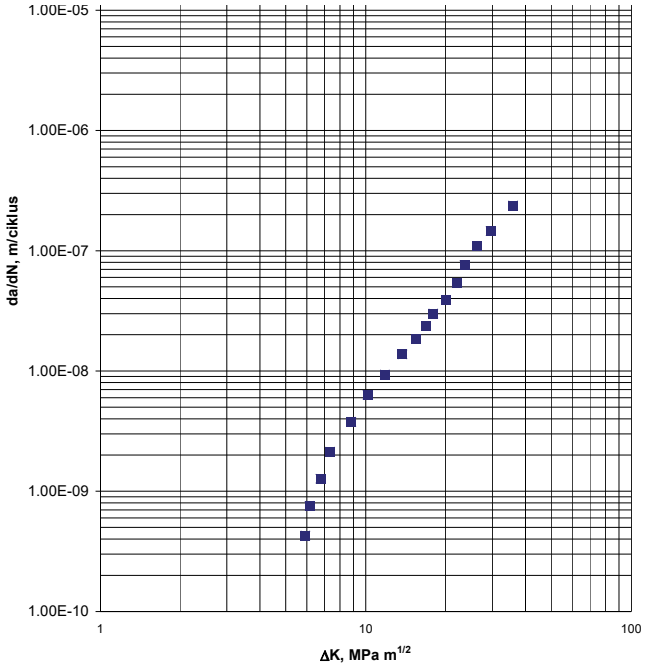

Figure 1: Diagram da/dN-K for specimen PM-1-1n, 20°C.

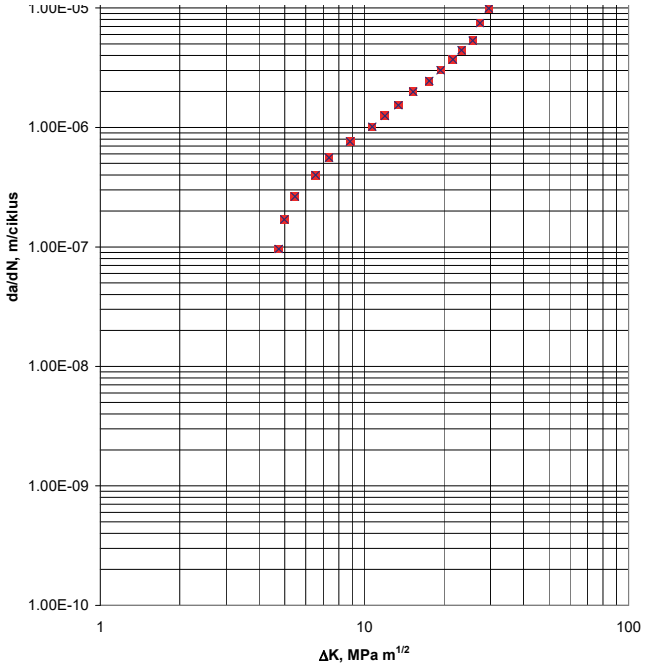

Figure 2: Diagram da/dN-K for specimen PM-2-1e, 540°C.

Obtained values for parameters of Paris law, $\frac{da}{dN} = C \cdot (\Delta K)^m$, i.e. coefficient C and exponent m, fatigue threshold ΔK_{th}, and fatigue crack growth rate, da/dN, for ΔK = 10 MPa$\sqrt{}$m, are given in Tabs. 5-9 for new and exploited PM, for new WM, and for new and exloited HAZ, respectively.

Specimen	Temperature °C	Fatigue threshold ΔK_{th}	Coefficient C	Exponent m	da/dN. m/cycle $\Delta K = 10$ MPa$\sqrt{m}$
PM-1-1n		5.9	$5.70 \cdot 10^{-12}$	2.98	$5.44 \cdot 10^{-9}$
PM-1-2n	20	5.6	$5.38 \cdot 10^{-12}$	3.02	$5.63 \cdot 10^{-9}$
PM-1-3n		5.8	$6.23 \cdot 10^{-12}$	2.83	$4.21 \cdot 10^{-9}$
PM-2-1n		5.2	$1.52 \cdot 10^{-10}$	2.94	$1.32 \cdot 10^{-7}$
PM-2-2n	540	5.1	$2.08 \cdot 10^{-10}$	2.88	$1.58 \cdot 10^{-7}$
PM-2-3n		5.0	$1.11 \cdot 10^{-10}$	2.99	$1.08 \cdot 10^{-7}$

Table 5: Fatigue crack growth parameters for specimens with notches in new PM.

Specimen	Temperature °C	Fatigue threshold ΔK_{th}	Coefficient C	Exponent m	da/dN. m/cycle $\Delta K = 10$ MPa$\sqrt{m}$
PM-1-1e		5.2	$4.45 \cdot 10^{-12}$	3.76	$2.56 \cdot 10^{-8}$
PM-1-2e	20	5.1	$3.89 \cdot 10^{-12}$	3.87	$2.88 \cdot 10^{-8}$
PM-1-3e		5.2	$5.17 \cdot 10^{-12}$	3.71	$2.65 \cdot 10^{-8}$
PM-2-1e		4.7	$1.48 \cdot 10^{-8}$	1.80	$9.34 \cdot 10^{-7}$
PM-2-2e	540	4.6	$2.67 \cdot 10^{-8}$	1.68	$1.28 \cdot 10^{-6}$
PM-2-3e		4.7	$1.25 \cdot 10^{-8}$	1.84	$8.65 \cdot 10^{-7}$

Table 6: Fatigue crack growth parameters for specimens with notches in exploited PM.

Specimen	Temperature °C	Fatigue threshold ΔK_{th}	Coefficient C	Exponent m	da/dN. m/cycle $\Delta K = 10$ MPa$\sqrt{m}$
WM-1-1e		6.8	$2.14 \cdot 10^{-11}$	2.53	$7.25 \cdot 10^{-9}$
WM-1-2e	20	6.9	$3.55 \cdot 10^{-11}$	2.38	$8.71 \cdot 10^{-9}$
WM-1-3e		6.7	$1.98 \cdot 10^{-11}$	2.56	$7.19 \cdot 10^{-9}$
WM-2-1e		5.8	$1.26 \cdot 10^{-9}$	2.51	$4.08 \cdot 10^{-7}$
WM-2-2e	540	5.6	$1.78 \cdot 10^{-9}$	2.47	$5.25 \cdot 10^{-7}$
WM-2-3e		5.5	$2.24 \cdot 10^{-9}$	2.21	$3.63 \cdot 10^{-7}$

Table 7: Fatigue crack growth parameters for specimens with notches in WM.

Specimen	Temperature °C	Fatigue threshold ΔK_{th}	Coefficient C	Exponent m	da/dN. m/cycle $\Delta K = 10$ MPa$\sqrt{m}$
HAZ-1-1n		5.7	$2.55 \cdot 10^{-11}$	2.48	$7.70 \cdot 10^{-9}$
HAZ-1-2n	20	5.4	$2.97 \cdot 10^{-11}$	2.41	$7.63 \cdot 10^{-9}$
HAZ-1-3n		5.5	$2.08 \cdot 10^{-11}$	2.57	$7.72 \cdot 10^{-9}$
HAZ-2-1n		4.9	$9.61 \cdot 10^{-10}$	2.47	$2.84 \cdot 10^{-7}$
HAZ-2-2n	540	4.7	$7.45 \cdot 10^{-10}$	2.83	$5.03 \cdot 10^{-7}$
HAZ-2-3n		4.8	$8.85 \cdot 10^{-10}$	2.68	$4.24 \cdot 10^{-7}$

Table 8: Fatigue crack growth parameters for specimens with notches in new HAZ.

Specimen	Temperature °C	Fatigue threshold ΔK_{th}	Coefficient C	Exponent m	da/dN. m/cycle $\Delta K = 10$ MPa$\sqrt{m}$
HAZ-1-1e		4.8	$1.54 \cdot 10^{-10}$	2.62	$6.42 \cdot 10^{-8}$
HAZ-1-2e	20	4.6	$1.95 \cdot 10^{-10}$	2.57	$7.24 \cdot 10^{-8}$
HAZ-1-3e		4.5	$2.35 \cdot 10^{-10}$	2.51	$7.60 \cdot 10^{-8}$
HAZ-2-1e		4.2	$5.50 \cdot 10^{-9}$	2.33	$1.18 \cdot 10^{-6}$
HAZ-2-2e	540	4.1	$4.67 \cdot 10^{-9}$	2.49	$1.44 \cdot 10^{-6}$
HAZ-2-3e		4.3	$6.24 \cdot 10^{-9}$	2.11	$8.04 \cdot 10^{-7}$

Table 9: Fatigue crack growth parameters for specimens with notches in exploited HAZ.

Influence of testing temperature and exploitation period on the fatigue threshold ΔK_{th} is graphically presented in Fig. 3-5, for PM, WM and HAZ, respectively.

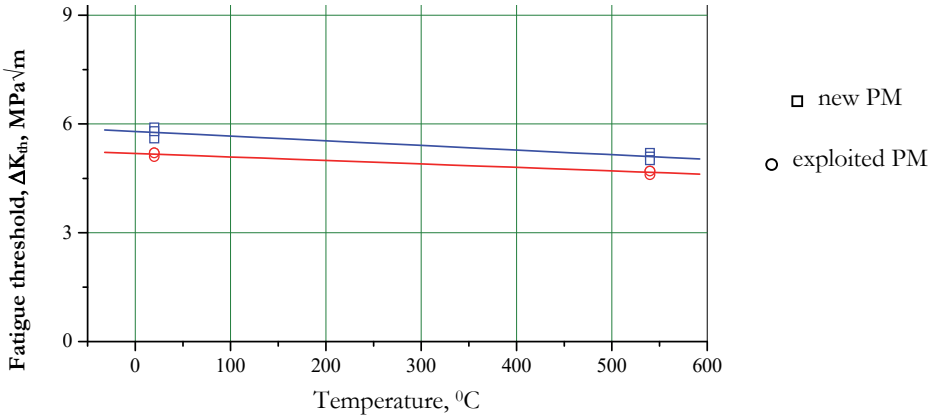

Figure 3: Fatigue threshold ΔK_{th} vs. temperature in PM

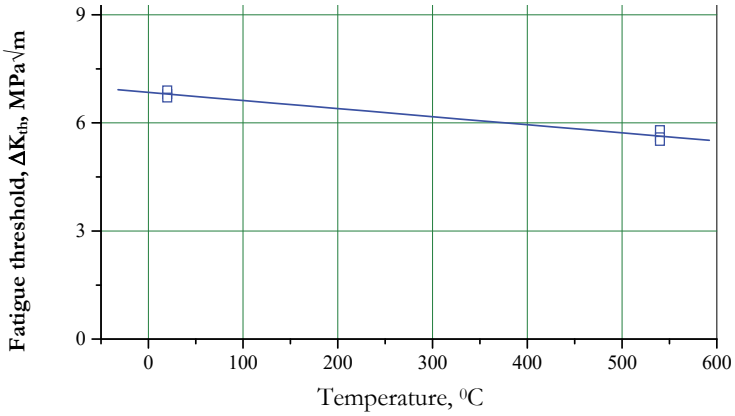

Figure 4: Fatigue threshold ΔK_{th} vs. temperature in WM.

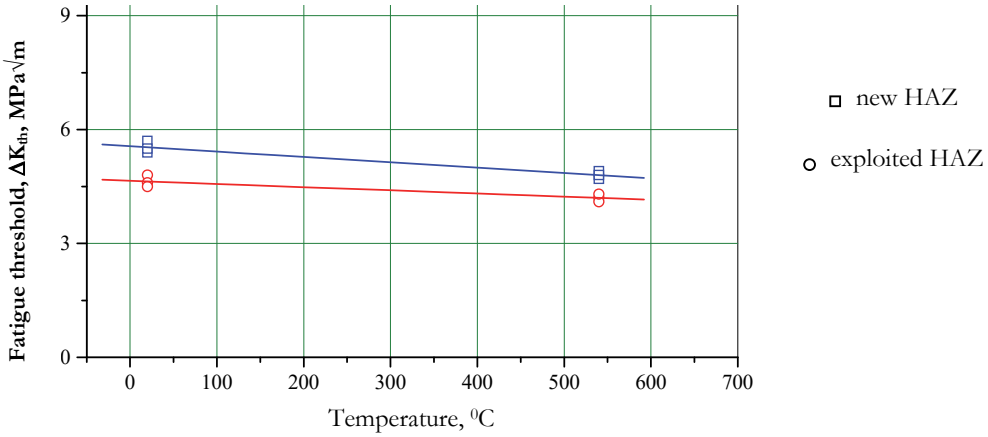

Figure 5: Fatigue threshold ΔK_{th} vs. temperature in HAZ.

The influence of testing temperature and exploitation period on the fatigue crack growth rate, da/dN, is graphically presented in Fig. 6-8, for PM, WM and HAZ, respectively.

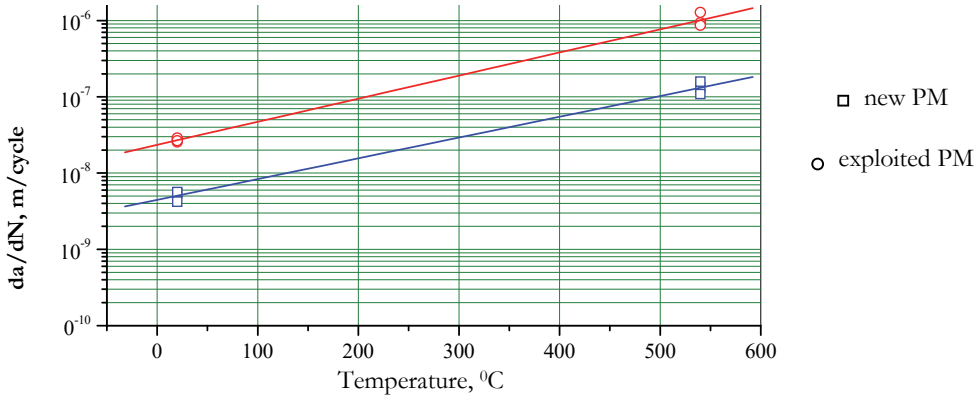

Figure 6: Fatigue crack growth rate, da/dN, vs. temperature for specimens with notches in PM.

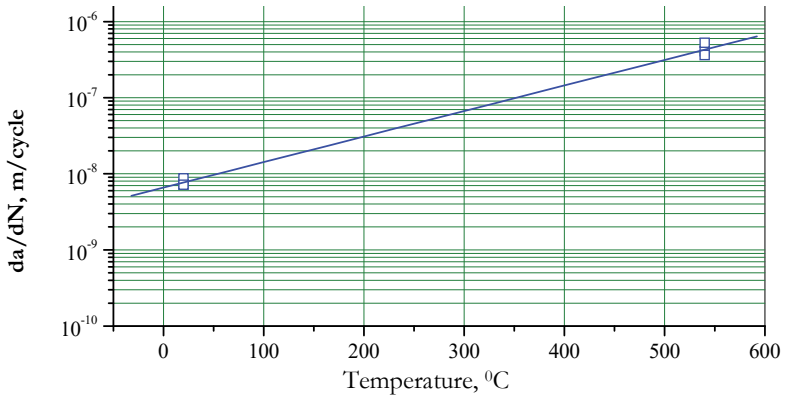

Figure 7: Fatigue crack growth rate, da/dN, vs. temperature for specimens with notches in WM.

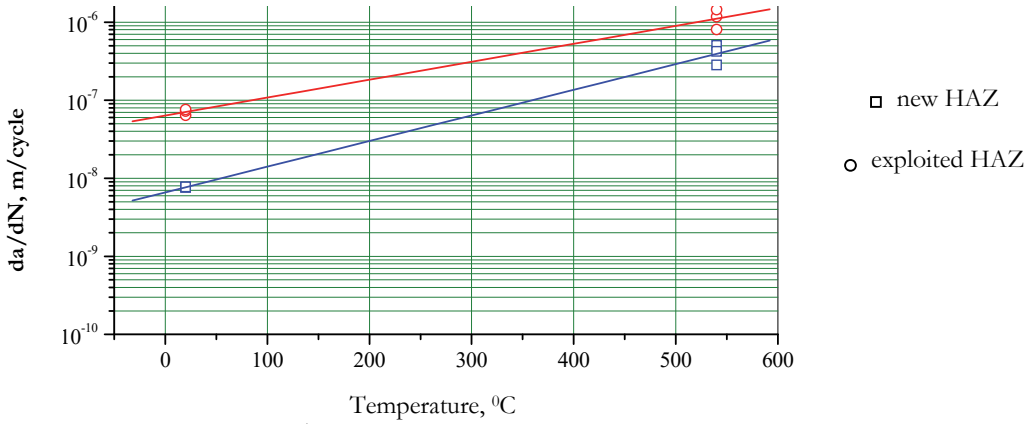

Figure 8: Fatigue crack growth rate, da/dN, vs. temperature for specimens with notches in HAZ.

Discussion

Values obtained for PM fatigue threshold, ΔK_{th}, are in the range 5.8 MPa√m (20 °C) to 5.1 MPa√m (540 °C), Tab. 5. Additional reduction for 10-15% is recorded due to exploition period 10-15%, since values for fatigue threshold, ΔK_{th}, are in that case in the range 5.2 MPa√m (20 °C) to 4.7 MPa√m (540 °C), Tab. 6. Similar effects are noticed in HAZ, where values of fatigue threshold, ΔK_{th}, obtained for new material, are in the range 5.5 MPa√m (20 °C) to 4.8 MPa√m (540 °C), i.e. from 4.6 MPa√m (20 °C) to 4.2 MPa√m (540 °C) for exploited material, Tabs. 8 and 9.

The largest values of fatigue threshold, ΔK_{th}, are obtianed in WM, from 6.8 MPa√m (20 °C) to 5.6 MPa√m (540 °C), Tab. 7.

Fatigue crack growth rate, da/dN, increases with temperature, being in the range $5.09 \cdot 10^{-9}$ m/cycle for new PM (20 °C) to $1.33 \cdot 10^{-7}$ m/cycle (540 °C), Tab. 5. Exploition period additionally increases fatigue crack growth rate, da/dN, from $2.70 \cdot 10^{-8}$ m/cycle (20 °C) to $1.03 \cdot 10^{-6}$ m/cycle (540 °C), Tab. 6. The same holds for HAZ, where values of fatigue crack growth rate, da/dN, are in the range $7.68 \cdot 10^{-9}$ m/cycle (20 °C) to $4.04 \cdot 10^{-7}$ m/cycle (540 °C) for new material, i.e. in the range $7.09 \cdot 10^{-8}$ m/cycle (20 °C), to $1.14 \cdot 10^{-6}$ m/cycle (540°C) for exploited material, Tabs. 8 and 9, respectivley. One should notice significantly higher values for fatigue crack growth rate in HAZ as compared to PM. The values for WM are in between, in the range $7.72 \cdot 10^{-9}$ m/cycle (20 °C) to $4.32 \cdot 10^{-7}$ m/cycle (540°C), Tab. 7.

CONCLUSION

Based on the presented results, one can conclude the following:

- Influence of material heterogeneity, as well as temperature and exploation effects, on fatigue threshold, da/dN, and crack growth rate, da/dN, is significant.
- Fatigue threshold values are the lowest for WM, and lowest for HAZ, whereas crack growth rate values are highest for HAZ and lowest for PM. Therefore, generally speaking, the lowest fatigue crack resistance is in HAZ.
- Higher temperature and longer exploitation peroids increase crack growth rates and decreases fatigue thresholds for both new and exploited materials in all regions of welded joint (PM, WM, HAZ). These effects are due to microstructural changes such as carbide formation and growth at grain boundaries and inside grains.

REFERENCES

[1] Čamagić, I., Investigation of the effects of exploitation conditions on the structural life and integrity assessment of pressure vessels for high temperatures (in Serbian), doctoral thesis, University of Pristina, Faculty of Technical Sciences with the seat in Kosovska Mitrovica, (2013).

[2] Čamagić, I., Vasić, N., Jović, S., Burzić, Z., Sedmak, A., Influence of temperature and exploitation time on tensile properties and microstructure of specific welded joint zones, In: 5th International Congress of Serbian Society of Mechanics Arandjelovac, Serbia, (2015).

[3] ASTM E399-89, Standard Test Method for Plane-Strain Fracture Toughness of Metallic Materials, Annual Book of ASTM Standards, 03.01 (1986) 522.

[4] BS 7448-Part 1, Fracture mechanics toughness tests-Method for determination of K_{Ic} critical CTOD and critical J values of metallic materials, BSI, (1991).